

Two-Baryon Systems with Twisted Boundary Conditions

Raúl A. Briceño^{*},¹ Zohreh Davoudi^{†,2,3} Thomas C. Luu^{‡,4,5} and Martin J. Savage^{§2,3}

¹*Jefferson Laboratory, 12000 Jefferson Avenue, Newport News, VA 23606, USA*

²*Department of Physics, University of Washington, Box 351560, Seattle, WA 98195, USA*

³*Institute for Nuclear Theory, Box 351550, Seattle, WA 98195-1550, USA*

⁴*Institute for Advanced Simulation, Forschungszentrum Jülich, D-52425 Jülich, Germany*

⁵*Institut für Kernphysik and Jülich Center for Hadron Physics,
Forschungszentrum Jülich, D-52425 Jülich, Germany*

(Dated: February 17, 2022)

We explore the use of twisted boundary conditions in extracting the nucleon mass and the binding energy of two-baryon systems, such as the deuteron, from Lattice QCD calculations. Averaging the results of calculations performed with periodic and anti-periodic boundary conditions imposed upon the light-quark fields, or other pair-wise averages, improves the volume dependence of the deuteron binding energy from $\sim e^{-\kappa L}/L$ to $\sim e^{-\sqrt{2}\kappa L}/L$. However, a twist angle of $\pi/2$ in each of the spatial directions improves the volume dependence from $\sim e^{-\kappa L}/L$ to $\sim e^{-2\kappa L}/L$. Twist averaging the binding energy with a random sampling of twist angles improves the volume dependence from $\sim e^{-\kappa L}/L$ to $\sim e^{-2\kappa L}/L$, but with a standard deviation of $\sim e^{-\kappa L}/L$, introducing a signal-to-noise issue in modest lattice volumes. Using the experimentally determined phase shifts and mixing angles, we determine the expected energies of the deuteron states over a range of cubic lattice volumes for a selection of twisted boundary conditions.

I. INTRODUCTION

Lattice quantum chromodynamics (LQCD) is evolving into a quantitative tool with which to describe the low-energy dynamics of few-body hadronic systems. After fully quantifying both the statistical and systematic uncertainties that are inherent in LQCD calculations, the masses of the lowest-lying hadrons are found to be in impressive agreement with those of nature [1, 2]. Recently, the ground-state energies of the s-shell nuclei and hypernuclei have been determined at a small number of light-quark masses [3–10]. Through algorithmic improvements, along with the growth in available computational resources, such calculations are moving towards the physical values of quark masses, and to calculations of nuclear properties such as magnetic moments. It is exciting to realize that within the next few years, LQCD calculations will provide a firm foundation for the forces between nucleons directly from QCD, e.g. Ref. [11]. One of the few systematic uncertainties present in the results of LQCD calculations arises in the infinite-volume extrapolation from finite-spacetime lattices, which, in fact, can be quantified by performing calculations in a range of lattice volumes. For simple systems such as $\pi^+\pi^+$ [12, 13], using effective field theory (EFT) methods, or direct knowledge of the S-matrix, the functional volume dependence of observables is available to provide well-defined predictions in infinite volume.

The finite-volume (FV) corrections to the mass of hadrons are dominated by the pion mass, m_π , and for a cubic volume with the spatial extent L the leading order (LO) corrections scale as $e^{-m_\pi L}/L$ [14]. For two-body bound states, the size of the bound state provides a second scale

^{*} rbriceno@jlab.org

[†] davoudi@uw.edu

[‡] t.luu@fz-juelich.de

[§] mjs5@uw.edu

responsible for volume modifications. These scale as $e^{-\kappa L}/L$ at LO in the volume expansion [15, 16], where κ is the binding momentum of the bound state comprised of two particles of masses m_1 and m_2 with a binding energy of $B = -(\sqrt{-\kappa^2 + m_1^2} + \sqrt{-\kappa^2 + m_2^2} - m_1 - m_2)$. For the deuteron, which is the only two-nucleon bound state in nature and is bound by only $B_d^\infty = 2.224644(34)$ MeV, these latter volume corrections can be large even in a modest lattice volume for generic boundary conditions (BCs) imposed upon the quark fields. As an example, an extraction of the deuteron binding energy that is accurate at the percent level from quark fields subject to periodic boundary conditions (PBCs) requires volumes with $L \gtrsim 17$ fm. However, this is the worst-case scenario as, for instance, also producing correlation functions corresponding to a non-zero center-of-mass (CM) momentum allows for an exponential reduction in the volume dependence [17, 18]. Such calculations will permit single-volume determinations of the deuteron binding energy with percent-level accuracy in significantly smaller volumes.

LQCD calculations are commonly performed with PBCs imposed upon the quark fields in the spatial directions, constraining the quark momentum modes in the volume to satisfy $\mathbf{p} = \frac{2\pi}{L}\mathbf{n}$ with \mathbf{n} being an integer triplet. PBCs are a subset of a larger class of BCs called twisted BCs (TBCs). TBCs [19] are those that require the quark fields to acquire a phase θ at the boundary, $\psi(\mathbf{x} + \mathbf{n}L) = e^{i\theta \cdot \mathbf{n}}\psi(\mathbf{x})$, where $0 < \theta_i < 2\pi$ is the twist angle in the i^{th} Cartesian direction. Bedaque [20] introduced this idea to the LQCD community, and showed that TBCs are equivalent to having a $U(1)$ background gauge field in the QCD Lagrangian with the quarks subject to PBCs. An arbitrary momentum can be selected for a (non-interacting) hadron by a judicious choice of the twist angles of its valence quarks, $\mathbf{p} = \frac{2\pi}{L}\mathbf{n} + \frac{\boldsymbol{\phi}}{L}$, where $\boldsymbol{\phi}$ is the sum of the twists of the valence quarks, again with $0 < \phi_i < 2\pi$, and \mathbf{n} is an integer triplet. TBCs have been shown to be useful in LQCD calculations of the low-momentum transfer behavior of form factors required in determining hadron radii and moments, circumventing the need for large-volume lattices [21–28]. They have also been speculated to be helpful in calculations of $K \rightarrow \pi\pi$ decays by bringing the initial and final FV states closer in energy [29, 30].

In addition to performing calculations with a particular twist, by averaging the results of calculations over twist angles, the discrete sum over momentum modes becomes an integral over momenta,

$$\int \frac{d^3\phi}{(2\pi)^3} \frac{1}{L^3} \sum_{\mathbf{n} \in \mathbb{Z}^3} \equiv \int \frac{d^3\mathbf{p}}{(2\pi)^3} \quad . \quad (1)$$

Although the volume dependence of most quantities is non linear due to interactions, such averaging can eliminate significant FV effects. This was first examined in the context of condensed-matter physics where, for example, the finite-size effects in the finite-cluster calculations of correlated electron systems are shown to be reduced by the boundary condition integration technique [31, 32]. This technique is implemented in quantum Monte Carlo (QMC) algorithms of many-body systems, and results in faster convergence of energies to the thermodynamic limit [33].

In this paper, we discuss the advantages of using TBCs to reduce the FV modifications to the mass of hadrons and to the binding energy of two-hadron bound states, such as the deuteron. In particular, we consider the FV effects resulting from averaging the results obtained from PBC and anti-PBCs (APBCs), from a specific choice of the twist angle, i-PBCs, and from averaging over twist angles. For the two-nucleon systems, the volume improvement is explored both analytically and numerically with the use of the recently developed FV formalism for nucleon-nucleon (NN) systems that is generalized to systems with TBCs. As was first noted by Bedaque and Chen [34], the need to generate new gauge field configurations with fully twisted BCs can be circumvented by imposing TBCs on the valence quarks only, which defines partial twisting. Partial twisting gives rise to corrections beyond full twisting that scale as $e^{-m_\pi L}/L$, and can be neglected for sufficiently large volumes compared to the FV effects from the size of weakly bound states. Although the

validity of partial twisting makes it feasible to achieve an approximate twist-averaged result in LQCD calculations, this remains a computationally expensive technique. We demonstrate that certain hadronic twist angles can result in an exponentially-improved convergence to the infinite-volume limit of certain quantities, with an accuracy that is comparable to the twist-averaged mean. Further, we speculate that similar improvements are also present in arbitrary n -body systems.

In some situations it is desirable to keep the volume finite as the extraction of physical quantities relies on non-vanishing FV effects. This is the well-known Lüscher methodology [15, 35], where the $2 \rightarrow 2$ elastic scattering amplitude can be obtained from the discrete energy eigenvalues of the two particles in a FV (see also Refs. [16–18, 36–55] for various extensions of the Lüscher formula). A prominent example, as discussed in Refs. [18, 56], is the FV analysis of the two-nucleon system in the 3S_1 - 3D_1 coupled channels. The ability to extract the S - D mixing parameter, ϵ_1 , and consequently the D/S ratio of the deuteron, depends upon the FV modifications to the binding energy when the deuteron is boosted in particular directions within the lattice volume [18]. The use of TBCs will further enhance the effectiveness of such calculations. By appropriate choices of the twist angles of each hadron, different CM energies can be accessed in a single lattice volume, further constraining the scattering parameters with the use of Lüscher’s method (see e.g. Refs. [57–60] for demonstrations of this technique in studying hadronic resonances). Due to the possibility of partial twisting in NN scattering, these extra energy levels can be obtained without having to generate additional ensembles of gauge-field configurations, in analogy with the boosted calculations (this technique has recently been used to calculate J/ψ - ϕ scattering [60]). Of course, the spectra of energy eigenvalues determined with a range of twist angles allow for fits to parametrizations of the S-matrix elements, which can then be used to predict infinite-volume quantities, such as binding energies [61, 62]. TBCs provide a way to reduce the systematic uncertainties that are currently present in analyses of coupled-channels systems by providing the ability to control, at some level, the location of eigenstates.

II. THE NUCLEON

If the up and down quarks have distinct twist angles, the charged pions, the proton and the neutron will acquire net twist angles denoted as $\phi^{\pi^+} = -\phi^{\pi^-}$, ϕ^p and ϕ^n , respectively, while the flavor-singlet mesons, such as π^0 , will remain untwisted, $\phi^{\pi^0} = \mathbf{0}$. The optimal set of quark twists depends upon the desired observable, and an appropriate choice can yield a relation between the twists of different hadrons, or leave a hadron untwisted.



FIG. 1: Leading loop contributions to the mass of the nucleon. The solid line, solid-double line and dashed line denote a nucleon, a Δ resonance and a pion, respectively. The black disks denote axial couplings.

The FV corrections to the mass of nucleon M_N , in a cubic volume with PBCs imposed on the quark fields, have been calculated at one-loop order in two-flavor baryon χ PT [63, 64] (the three-flavor result can be found in Ref. [65]). Including Δ resonance as a degree of freedom, these

corrections are obtained from the diagrams in Fig. 1, and take the form [64]¹

$$\delta_L M_N \equiv M_N(L) - M_N(\infty) = \frac{3g_A^2}{8\pi^2 f_\pi^2} \mathcal{K}(0) + \frac{g_{\Delta N}^2}{3\pi^2 f_\pi^2} \mathcal{K}(\Delta) \quad , \quad (2)$$

where

$$\mathcal{K}(0) = \frac{\pi}{2} m_\pi^2 \sum_{\mathbf{n} \neq 0} \frac{e^{-|\mathbf{n}|m_\pi L}}{|\mathbf{n}|L} \quad , \quad (3)$$

and

$$\mathcal{K}(\Delta) = \int_0^\infty d\lambda \beta_\Delta \sum_{\mathbf{n} \neq 0} \left[\beta_\Delta K_0(\beta_\Delta |\mathbf{n}|L) - \frac{1}{|\mathbf{n}|L} K_1(\beta_\Delta |\mathbf{n}|L) \right] \quad . \quad (4)$$

m_π and f_π are the pion mass and decay constant, and g_A and $g_{\Delta N}$ denote the nucleon axial charge and the Δ -nucleon coupling constant, respectively. $K_n(z)$ is the modified Bessel function of the second kind. $\beta_\Delta = \lambda^2 + 2\lambda\Delta + m_\pi^2$ where Δ denotes the nucleon- Δ mass splitting. When expanded in the limit of large L , Eq. (2) scales as $e^{-m_\pi L}/L$ at LO.

Heavy baryon χ PT (HB χ PT) has been used to calculate the masses of the proton and neutron in a FV at the one-loop level with TBCs [66].² The Poisson re-summation formula makes it possible to factor the dependences on the twist angles as pure phases, allowing the expressions for the masses to be put into a simple form. The proton mass is found to be

$$\delta_L M_p = \frac{g_A^2}{4\pi^2 f_\pi^2} \mathcal{K}^p(0; \phi^\pi) + \frac{g_{\Delta N}^2}{6\pi^2 f_\pi^2} \mathcal{K}^p(\Delta; \phi^\pi) \quad , \quad (5)$$

where

$$\mathcal{K}^p(0; \phi^\pi) = \frac{\pi}{2} m_\pi^2 \sum_{\mathbf{n} \neq 0} \frac{e^{-|\mathbf{n}|m_\pi L}}{|\mathbf{n}|L} \left(\frac{1}{2} + e^{-i\mathbf{n} \cdot \phi^{\pi^+}} \right) \quad , \quad (6)$$

and

$$\begin{aligned} \mathcal{K}^p(\Delta; \phi^\pi) = \int_0^\infty d\lambda \beta_\Delta \sum_{\mathbf{n} \neq 0} & \left[\beta_\Delta K_0(\beta_\Delta |\mathbf{n}|L) - \frac{1}{|\mathbf{n}|L} K_1(\beta_\Delta |\mathbf{n}|L) \right] \\ & \times (e^{-i\mathbf{n} \cdot \phi^{\pi^-}} + \frac{2}{3} + \frac{1}{3} e^{-i\mathbf{n} \cdot \phi^{\pi^+}}) \quad , \end{aligned} \quad (7)$$

and the neutron mass can be found from these expressions by the substitutions $p \rightarrow n$ and $\pi^+ \leftrightarrow \pi^-$. It is convenient to consider the periodic images associated with the nucleon having their contributions modified by the appropriate phase factor due to the TBCs.

After twist averaging (over the twists of the pion field, see Appendix A), the leading FV corrections to the mass of both the proton and the neutron arising from Eq. (5) are 1/3 of their value when calculated with PBCs, Eq. (2).³ Of course, calculations at multiple twist angles need not be performed to estimate the twist-averaged value, and special twist angles can be selected based

¹ Note that we have chosen to define the $\mathcal{K}(\Delta)$ function with a negative sign compared to Ref. [64].

² The FV corrections to meson masses, decay constants and semileptonic form factors with both the TBCs and the partially-TBCs have been calculated at LO in χ PT in Ref. [30].

³ If the twist of the up and down quarks is the same, ϕ^{π^\pm} vanishes and no volume improvement will be obtained by averaging.

upon the symmetries of the integer sums in Eqs. (6) and (7).⁴ In particular, it is notable that the leading volume effects of the form $e^{-m_\pi L}/L$, $e^{-\sqrt{2}m_\pi L}/L$ and $e^{-\sqrt{3}m_\pi L}/L$, can be reduced by a factor of three with i-PBCs, by setting the pion twist angle to $\phi^{\pi^+} = (\frac{\pi}{2}, \frac{\pi}{2}, \frac{\pi}{2})$. Averaging the masses calculated with PBCs and APBCs also reduces the leading contribution by a factor of three. The leading volume dependence can be eliminated completely by choosing $\phi^{\pi^+} = (\frac{4\pi}{3}, \frac{4\pi}{3}, \frac{4\pi}{3})$, leaving volume corrections to the nucleon mass of the form $\sim e^{-\sqrt{2}m_\pi L}/L$. It is likely that optimal twists exist for other single nucleon properties, such as matrix elements of the isovector axial current, g_A .

For arbitrary quark twists, the proton and neutron have, in general, different phase spaces as the momentum modes that exist in the FV differ. As an example, while quark twists can be chosen to keep the proton at rest in the volume and allow for averaging over the charged pion twists, $\phi^{(d)} = -2\phi^{(u)}$, in general the neutron will have non-zero momentum.⁵

III. TWO BARYONS

The positive-energy eigenvalues of two hadrons in a FV subject to PBCs in the spatial directions exhibit power-law volume dependences, while the negative-energy eigenvalues deviate exponentially from their infinite-volume values. These energy eigenvalues can be related to the infinite-volume scattering amplitude below the inelastic threshold, with corrections that scale as $\sim e^{-m_\pi L}/L$ [15, 35] (see also Refs. [16, 45, 56, 71]). The S-wave NN energy quantization condition (QC) was generalized to systems with TBCs at rest in Ref. [20], and to more general two-hadron systems in Ref. [72]. Lüscher's energy QC [15, 35], which determines the form of the FV corrections, is dictated by the on-shell two-particle states within the volume. Once the kinematic constraints on the momentum modes of the two-particle states in the FV are determined, the corresponding QC can be determined in a straightforward manner. Explicitly, the QC is of the form

$$\det [(\mathcal{M}^\infty)^{-1} + \delta\mathcal{G}^V] = 0, \quad (8)$$

where \mathcal{M}^∞ is the infinite-volume scattering amplitude matrix evaluated at the on-shell momentum of each particle in the CM frame, p^* . For nonrelativistic systems, it is convenient to express the QC in the $|JM_J(LS)\rangle$ basis, where J is the total angular momentum, M_J is the eigenvalue of the \hat{J}_z operator, and L and S are the orbital angular momentum and the total spin of the system, respectively. The matrix elements of $\delta\mathcal{G}^V$ in this basis are⁶

$$\begin{aligned} [\delta\mathcal{G}^V]_{JM_J, LS; J'M'_J, L'S'} &= i\eta \frac{p^*}{8\pi E^*} \delta_{SS'} \left[\delta_{JJ'} \delta_{M_J M'_J} \delta_{LL'} + i \sum_{l,m} \frac{(4\pi)^{3/2}}{p^{*l+1}} c_{lm}^{\mathbf{d}, \phi_1, \phi_2}(p^{*2}; L) \right. \\ &\quad \times \sum_{M_L, M'_L, M_S} \langle JM_J | LM_L, SM_S \rangle \langle L'M'_L, SM_S | J'M'_J \rangle \int d\Omega Y_{LM_L}^* Y_{lm}^* Y_{L'M'_L} \left. \right], \quad (9) \end{aligned}$$

where $\eta = 1/2$ for identical particles and $\eta = 1$ otherwise, and $\langle JM_J | LM_L, SM_S \rangle$ are Clebsch-Gordan coefficients. E^* is the total CM energy of the system, $E^* = \sqrt{p^{*2} + m_1^2} + \sqrt{p^{*2} + m_2^2}$ where m_1 and m_2 are the masses of the particles, and ϕ_1 and ϕ_2 are their respective twist angles.

⁴ This technique is used to reduce the finite-size effects in QMC many-body calculations (commonly known as “special k-points”), as explored in Refs. [67–70].

⁵ Such non-trivial phase spaces somewhat complicate the analysis of LQCD calculations of multi-baryon systems.

⁶ This relation has been derived in Ref. [18] for two nucleons subject to PBCs. It reduces to the QC for meson-nucleon scattering [43] and to meson-meson scattering [15, 36, 39, 40]. For an alternate derivation, see Ref. [45].

The total momentum of the system is $\mathbf{P} = \frac{2\pi}{L}\mathbf{d} + \frac{\phi_1 + \phi_2}{L}$ with $\mathbf{d} \in \mathbb{Z}^3$. The volume dependence and the dependence on the BCs are in the kinematic functions $c_{lm}^{\mathbf{d}, \phi_1, \phi_2}(p^{*2}; L)$, defined as

$$c_{lm}^{\mathbf{d}, \phi_1, \phi_2}(p^{*2}; L) = \frac{\sqrt{4\pi}}{\gamma L^3} \left(\frac{2\pi}{L} \right)^{l-2} \mathcal{Z}_{lm}^{\mathbf{d}, \phi_1, \phi_2}[1; (p^* L/2\pi)^2] \quad , \quad (10)$$

with

$$\mathcal{Z}_{lm}^{\mathbf{d}, \phi_1, \phi_2}[s; x^2] = \sum_{\mathbf{r} \in \mathcal{P}_{\mathbf{d}, \phi_1, \phi_2}} \frac{|\mathbf{r}|^l Y_{lm}(\mathbf{r})}{(\mathbf{r}^2 - x^2)^s} \quad . \quad (11)$$

$\gamma = E/E^*$ where E is the total energy of the system in the rest frame of the volume (the lab frame), $E^2 = \mathbf{P}^2 + E^{*2}$. The sum in Eq. (11) is performed over the momentum vectors \mathbf{r} that belong to the set $\mathcal{P}_{\mathbf{d}, \phi_1, \phi_2}$, which remains to be determined.

Consider the two-hadron wavefunction in the lab frame [17, 36] that is subject to the TBCs,

$$\psi_{\text{Lab}}(\mathbf{x}_1 + L\mathbf{n}_1, \mathbf{x}_2 + L\mathbf{n}_2) = e^{i\phi_1 \cdot \mathbf{n}_1 + i\phi_2 \cdot \mathbf{n}_2} \psi_{\text{Lab}}(\mathbf{x}_1, \mathbf{x}_2) \quad , \quad (12)$$

where \mathbf{x}_1 and \mathbf{x}_2 denote the position of the hadrons, and $\mathbf{n}_1, \mathbf{n}_2 \in \mathbb{Z}^3$. As the total momentum of the system is conserved, the wavefunction can be written as an eigenfunction of the total momentum $P = (E, \mathbf{P})$. In the lab frame, the equal-time wavefunction of the system is

$$\psi_{\text{Lab}}(x_1, x_2) = e^{-iEX^0 + i\mathbf{P} \cdot \mathbf{X}} \varphi_{\text{Lab}}(0, \mathbf{x}_1 - \mathbf{x}_2) \quad , \quad (13)$$

where the position of the CM is X , and

$$X = \alpha x_1 + (1 - \alpha)x_2 \quad , \quad \alpha = \frac{1}{2} \left(1 + \frac{m_1^2 - m_2^2}{E^{*2}} \right) \quad , \quad (14)$$

for systems with unequal masses [17]. Since the CM wavefunction is independent of the relative time coordinate [36], $\varphi_{\text{Lab}}(0, \mathbf{x}_1 - \mathbf{x}_2) = \varphi_{\text{CM}}(\hat{\gamma}(\mathbf{x}_1 - \mathbf{x}_2))$, where the boosted relative position vector is $\hat{\gamma}\mathbf{x} = \gamma\mathbf{x}_{\parallel} + \mathbf{x}_{\perp}$, with \mathbf{x}_{\parallel} (\mathbf{x}_{\perp}) the component of \mathbf{x} that is parallel (perpendicular) to \mathbf{P} . By expressing ψ_{Lab} in Eq. (12) in terms of φ_{CM} , it straightforwardly follows that

$$e^{i\alpha\mathbf{P} \cdot (\mathbf{n}_1 - \mathbf{n}_2)L + i\mathbf{P} \cdot \mathbf{n}_2 L} \varphi_{\text{CM}}(\mathbf{y}^* + \hat{\gamma}(\mathbf{n}_1 - \mathbf{n}_2)L) = e^{i\phi_1 \cdot \mathbf{n}_1 + i\phi_2 \cdot \mathbf{n}_2} \varphi_{\text{CM}}(\mathbf{y}^*) \quad , \quad (15)$$

where $\mathbf{y}^* = \mathbf{x}_1^* - \mathbf{x}_2^*$ is the relative coordinate of two hadrons in the CM frame. By Fourier transforming this relation, and using the form of the total momentum \mathbf{P} from above, the relative momenta allowed in the FV energy QC are constrained to be

$$\mathbf{r} = \frac{1}{L} \hat{\gamma}^{-1} \left[2\pi(\mathbf{n} - \alpha\mathbf{d}) - (\alpha - \frac{1}{2})(\phi_1 + \phi_2) + \frac{1}{2}(\phi_1 - \phi_2) \right] \quad , \quad (16)$$

where $\mathbf{n} \in \mathbb{Z}^3$ is summed over in Eq. (11). These results encapsulate those of Refs. [17, 36, 46, 47, 50] when the PBCs are imposed, i.e., when $\phi_1 = \phi_2 = \mathbf{0}$. It also recovers two limiting cases that are considered in Ref. [72] for the use of TBCs in the scalar sector of QCD. It should be noted that for particles with equal masses, $\alpha = 1/2$, the set of allowed momentum vectors reduces to

$$\mathbf{r} = \frac{1}{L} \hat{\gamma}^{-1} \left[2\pi(\mathbf{n} - \frac{1}{2}\mathbf{d}) + \frac{1}{2}(\phi_1 - \phi_2) \right] \quad . \quad (17)$$

It is important to note that for two identical hadrons, when $\phi_1 = \phi_2 = \phi$, the FV spectra show no non-trivial dependence on the twist other than a shift in the total energy of the system,

$E^2 = (\frac{2\pi}{L}\mathbf{d} + \frac{\phi}{L})^2 + E^{*2}$. As a result, twisting will not provide additional constraints on the scattering amplitude in, for instance, the 1S_0 nn or pp channels. This is also the case for the FV studies of NN scattering in the 3S_1 - 3D_1 coupled channels if the same twist is imposed on the up and down quarks.⁷

A. The Deuteron

The energy spectra of two nucleons with spin $S = 1$ in a FV subject to PBCs and with a range of CM momenta have been determined from the experimentally measured phase shifts and mixing angles [18]. In particular, the dependence of the bound-state spectra on the non-zero mixing angle between S and D waves, ϵ_1 , has been determined. As seen from Eq. (17), the effects of the twist angles $\frac{1}{2\pi}(\phi_1 - \phi_2) = (0, 0, 1), (1, 1, 0), (1, 1, 1)$ on the CM spectra are the same as those of (untwisted) boost vectors, \mathbf{d} , considered in Ref. [18]. Therefore, different TBCs can provide additional CM energies in a single volume, similar to boosted calculations, which can be used to better constrain scattering parameters and the S-matrix. However, twisting may be a more powerful tool as it provides access to a continuum of momenta.

If imposing TBCs on the quark fields would require the generation of new ensembles of gauge-field configurations, it would likely not be optimal to expend large computational resources on multiple twisted calculations. However, PBCs can be retained on the sea quarks and TBCs can be imposed only in the valence sector [34]. The reason for this is that there are no disconnected diagrams associated with the NN interactions.⁸ At the level of the low-energy EFT, this indicates that there are no intermediate s-channel diagrams in which a nucleon or meson containing a sea quark can go on-shell. Such off-mass-shell hadrons modify the NN interactions by $\sim e^{-m_\pi L}/L$, and do not invalidate the use of the QC in Eq. (8) with the partially-TBCs as long as the calculations are performed in sufficiently large volumes, $L \gtrsim 9$ fm.

One significant advantage of imposing TBCs is the improvement in the volume dependence of the deuteron binding energy. Although the formalism presented in the previous section can be used to fit to various scattering parameters [18] (and consequently determine the deuteron binding energy), we will show that with a judicious choice of twist angles, the extracted energies in future LQCD calculations should be close to the infinite-volume values, even in volumes as small as $\sim (9 \text{ fm})^3$.

As discussed in the previous section, the CM energy of the np system is sensitive to TBCs only if different twists are imposed upon the up and down quarks. This means that, even if exact isospin symmetry is assumed, the proton and the neutron will have different phase spaces due to the different BCs. By relaxing the interchangeability constraint on the np state, as required by the different phase spaces, the NN positive-parity channels will mix with the negative-parity channels. This admixture of parity eigenstates is entirely a FV effect induced by the boundary conditions, and does not require parity violation in the interactions, manifesting itself in non-vanishing $c_{lm}^{\mathbf{d}, \phi_1, \phi_2}$ functions for odd values of l . As such, the spin of the NN system is preserved.

The QC in Eq. (8) depends on S-matrix elements in all partial waves, however it can be truncated to include only channels with $L \leq 2$ (requiring $J \leq 3$) because of the reducing size of the low-energy phase shifts in the higher channels. For arbitrary twist angles, the truncated QC can be represented by a 27×27 matrix in the $|JM_J(LS)\rangle$ basis, the eigenvalues of which dictate the energy eigenvalues. Fits to the experimentally known phase shifts and mixing parameters [73–77] are used

⁷ This result differs somewhat from the conclusion of Ref. [20].

⁸ As recently demonstrated, disconnected diagrams will not hinder the use of partially-TBCs in studies of the scalar sector of QCD either [72]. The graded symmetry of “partially-quenched” QCD results in cancellations among contributions from intermediate non-valence mesons.

to extrapolate to negative energies [18] to provide the inputs into the truncated QC, from which the deuteron spectra in a cubic volume with TBCs are predicted. The scattering parameters entering the analysis are $\delta_{1\alpha}$, ϵ_1 , $\delta_{1\beta}$, $\delta^{(3P_0)}$, $\delta^{(3P_1)}$, $\delta^{(3P_2)}$, $\delta^{(3D_2)}$ and $\delta^{(3D_3)}$, where the Blatt-Biedenharn (BB) parameterization [78] is used in the $J = 1$ sector. The twist angles explored in this work are $\phi^p = -\phi^n \equiv \phi = (0, 0, 0)$ (PBCs), (π, π, π) (APBCs) and $(\frac{\pi}{2}, \frac{\pi}{2}, \frac{\pi}{2})$ (i-PBCs). At the level of the quarks, this implies that the twist angles of the (valence) up and down quarks are $\phi^u = -\phi^d = \phi$. We also set $\mathbf{d} = \mathbf{0}$ in Eq. (16) so that the np system is at rest in the lab frame. The reason for this choice of twist angles is that they (directly or indirectly) give rise a significant cancellation of the leading FV corrections to the masses of the nucleons, as shown in Sec. II. The number of eigenvalues of $(\mathcal{M}^\infty)^{-1} + \delta\mathcal{G}^V$, and their degeneracies, reflect the spatial-symmetry group of the FV. Calculations with $\phi = \mathbf{0}$ respect the cubic (O_h) symmetry, while for $\phi = (\frac{\pi}{2}, \frac{\pi}{2}, \frac{\pi}{2})$ the symmetry group is reduced to the C_{3v} point group.⁹ However, for $\phi = (\pi, \pi, \pi)$ the system has inversion symmetry, and respects the D_{3h} point symmetry [79]. By examining the transformation properties of the $c_{lm}^{\mathbf{d}, \phi_1, \phi_2}$ functions under the symmetry operations of these groups, certain relations are found for any given l . These relations, as well as the eigenvectors of the FV matrices, which are tabulated elsewhere [13, 15, 36, 56, 80, 81], can be used to block diagonalize the 27×27 matrix representation of the QCs, where each block corresponds to an irrep of the point-group symmetry of the system. For the selected twist angles, the QCs of the irreps of the corresponding point groups that have overlap with the deuteron are given in the Appendix B.

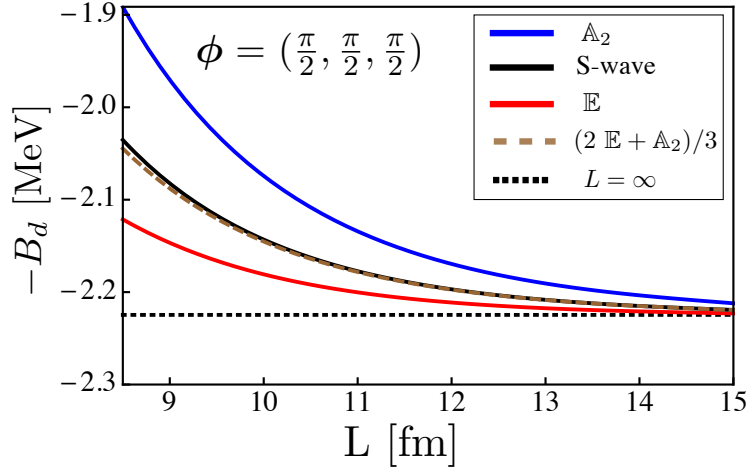


FIG. 2: The deuteron binding energy as a function of L using i-PBCs ($\phi^p = -\phi^n \equiv \phi = (\frac{\pi}{2}, \frac{\pi}{2}, \frac{\pi}{2})$). The blue curve corresponds to the \mathbb{A}_2 irrep of the C_{3v} group, while the red curve corresponds to the \mathbb{E} irrep. The brown-dashed curve corresponds to the weighted average of the \mathbb{A}_2 and \mathbb{E} irreps, $-\frac{1}{3}(2B_d^{(\mathbb{E})} + B_d^{(\mathbb{A}_2)})$, while the black-solid curve corresponds to the S-wave limit. The infinite-volume deuteron binding energy is shown by the black-dotted line.

For i-PBCs, there are two irreps of the C_{3v} group, namely the one-dimensional irrep \mathbb{A}_1 and the two-dimensional irrep \mathbb{E} , that have overlap with the 3S_1 - 3D_1 coupled channels. Fig. 2 shows the binding energy (the CM energy minus the rest masses of the nucleons), $-B_d = E^* - M_p - M_n$,

⁹ There is a correspondence between the FV spatial symmetry in twisted calculations with arbitrary twists $\phi^p \neq \phi^n$ and the FV symmetry in (boosted) NN calculations with PBCs when isospin breaking is considered. For example, the point symmetry group corresponding to twisted calculations with $\phi^p = -\phi^n = (0, 0, \frac{\pi}{2})$ and that of the physical np system with $\mathbf{P} = \frac{2\pi}{L}(0, 0, 1)$ with PBCs are both C_{4v} .

as a function of L corresponding to \mathbb{A}_2 irrep (blue curve) and \mathbb{E} irrep (red curve), obtained from the QCs in Eqs. (B5) and (B6). Even at $L \sim 9$ fm, the deuteron binding energies extracted from both irreps are close to the infinite-volume value. In particular, calculations in the \mathbb{E} irrep of the C_{3v} group provide a few percent-level accurate determination of the deuteron binding energy in this volume. The black-solid curve in Fig. 2 represents the S-wave limit of the interactions, when the S-D mixing parameter and all phase shifts except that in the S-wave are set equal to zero. The M'_J -averaged binding energy, $-\frac{1}{3}(2B_d^{(\mathbb{E})} + B_d^{(\mathbb{A}_2)})$, converges to this S-wave limit, as shown in Fig. 2 (the \mathbb{A}_2 irrep contains the $M'_J = 0$ state while \mathbb{E} contains the $M'_J = \pm 1$ states, where M'_J is the projection of total angular momentum along the twist direction). In order to appreciate the significance of calculations performed with the $\phi = (\frac{\pi}{2}, \frac{\pi}{2}, \frac{\pi}{2})$ twist angles, it is helpful to recall the deuteron binding energy obtained in calculations with PBCs. For PBCs, the only irrep of the cubic group that has overlap with the 3S_1 - 3D_1 coupled channels is the three-dimensional irrep \mathbb{T}_1 , Eq. (B4), and the corresponding binding energy is shown in Fig. 3(a) (green curve). As is well known, the binding energy deviates significantly from its infinite-volume value, such that the FV deuteron is approximately twice as bound as the infinite-volume deuteron at $L = 9$ fm. For APBCs, two irreps of the D_{3h} group overlap with the deuteron channel, \mathbb{A}_2 and \mathbb{E} (Eqs. (B7,B8)), and yield degenerate binding energies as shown in Fig. 3(a) (purple curves). As seen in Fig. 3(a), the deuteron becomes unbound over a range of volumes and asymptotes slowly to the infinite-volume limit. However, in analogy with the nucleon masses, the volume dependence of the deuteron binding energy is significantly reduced by averaging the results obtained with PBCs and APBCs, as shown in Fig. 3(a) (black-solid curve). Fig. 3(b) provides a magnified view of this averaged quantity (black-solid curve), where the two energy levels associated with i-PBCs are shown for comparison.

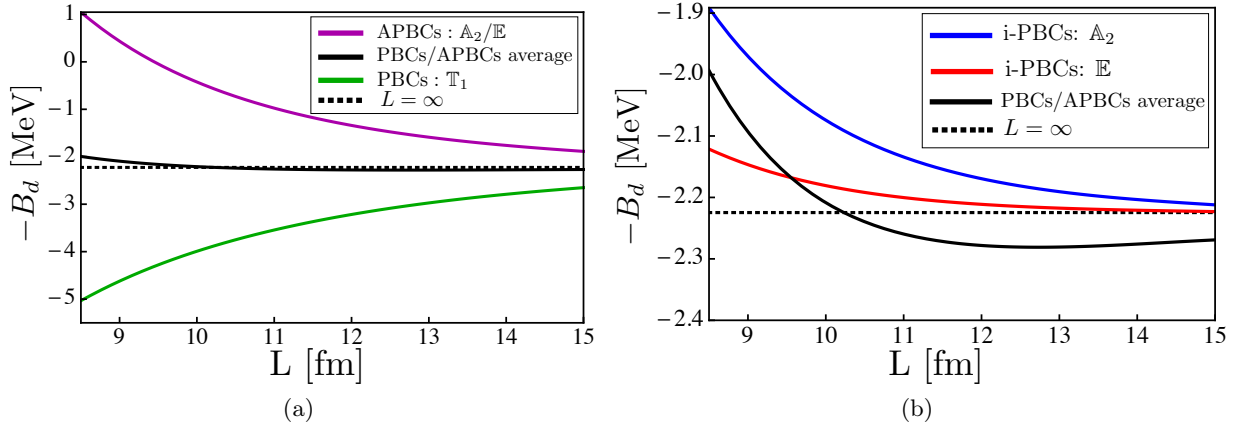


FIG. 3: a) The deuteron binding energy as a function of L from PBCs (green curve) and from APBCs (purple curve). The black-solid curve represents the average of these energies. b) A closer look at the average in part (a) compared with energies obtained with i-PBCs, \mathbb{A}_2 (blue curve) and \mathbb{E} (red curve).

In order to understand the observed volume improvements, consider the volume scaling of the full QC assuming that the phase shifts beyond the α -wave are small. In this limit, for a general set

of twist angles and boosts, the QC collapses to

$$\det \left[(p^* \cot \delta_{1\alpha} - 4\pi c_{00}) \begin{pmatrix} 1 & 0 & 0 \\ 0 & 1 & 0 \\ 0 & 0 & 1 \end{pmatrix} - \frac{2\pi}{\sqrt{5}p^{*2}} \left(\sqrt{2} \sin 2\epsilon_1 - \sin^2 \epsilon_1 \right) \begin{pmatrix} c_{20} & \sqrt{3}c_{21} & \sqrt{6}c_{22} \\ -\sqrt{3}c_{2-1} & -2c_{20} & -\sqrt{3}c_{21} \\ \sqrt{6}c_{2-2} & \sqrt{3}c_{2-1} & c_{20} \end{pmatrix} \right] = 0 \quad , \quad (18)$$

which depends upon the α -wave phase shift and the mixing parameter, ϵ_1 . Shorthand notation has been used for convenience, $c_{lm} = c_{lm}^{\mathbf{d}, \phi_1, \phi_2}(p^{*2}; L)$. For generic twist angles, deviations between the energy eigenvalues resulting from this truncated QC and the full QC scale as $\sim \tan \delta_i e^{-2\kappa L}/(\kappa L^2)$, where δ_i denotes phase shifts beyond the α -wave (see Appendix C for expansions of the $c_{lm}^{\mathbf{d}, \phi_1, \phi_2}$ functions). For i-PBCs, the leading corrections are from the P-waves, as can be seen from the expansions of the c_{lm} in Table C. By neglecting the small mixing between the S-wave and D-waves in Eq. (18), the QC dictated by S-wave interactions is ¹⁰

$$p^* \cot \delta^{(3S_1)}|_{p^*=i\kappa} + \kappa = \sum_{\mathbf{n} \neq \mathbf{0}} e^{i(\alpha - \frac{1}{2})\mathbf{n} \cdot (\phi^p + \phi^n)} e^{-i\frac{1}{2}\mathbf{n} \cdot (\phi^p - \phi^n)} e^{i2\pi\alpha\mathbf{n} \cdot \mathbf{d}} \frac{e^{-|\hat{\gamma}\mathbf{n}|\kappa L}}{|\hat{\gamma}\mathbf{n}|L} \quad . \quad (19)$$

The volume dependence of the deuteron binding momentum, κ , originates from the right-hand side of this equation. For $\mathbf{d} = \mathbf{0}$, the c_{2m} functions vanish for both PBCs and APBCs, leading to Eq. (19) without further approximation. For the twist angles $\phi^p = -\phi^n \equiv \phi = (\frac{\pi}{2}, \frac{\pi}{2}, \frac{\pi}{2})$ and boost $\mathbf{d} = \mathbf{0}$, the first few terms in the summation on the right-hand side of Eq. (19) ($\mathbf{n}^2 \leq 3$) vanish, leaving the leading volume corrections to scale as $\sim e^{-2\kappa L}/L$. A lesser cancellation occurs in the average of binding energies obtained with PBCs and APBCs, giving rise to deviations from the infinite-volume energy by terms that scale as $\sim e^{-\sqrt{2}\kappa L}/L$.

The result of Monte Carlo twist averaging of the deuteron binding energy can be ascertained from the behavior of the two extreme contributions, the PBC and APBC results. While the average binding energy obtained from N randomly selected sets of twist angles scales as $B_d^{(\infty)} + \mathcal{O}(e^{-2\kappa L}/L)$, the standard deviation of the mean scales as $\sim e^{-\kappa L}/(\sqrt{N}L)$, giving rise to a signal-to-noise in the binding energy that scales as $\sim \sqrt{N} B_d^{(\infty)} L e^{\kappa L}$, which even for $L \sim 14$ fm allows only for a poor extraction, as can be deduced from Fig. 3(a). It is clear that such a method is inferior to that of pair-wise averaging, such as from PBCs and APBCs, or choosing special twists, such as i-PBCs.

We have restricted ourselves to the scenarios where the net twist angles in each Cartesian direction (the lattice axes) are the same. One reason for this is that systems with arbitrary twists give rise to three distinct, but nearby, energy eigenvalues associated with combinations of each of the three M_J -states of the deuteron - a sub-optimal system to analyze in LQCD calculations. Another reason is that a twist of $\frac{\pi}{2}$ in each direction is optimal in minimizing the FV effects in both the two-body binding energies and the single-baryon masses. Further, averaging the results of calculations with PBCs and APBCs also eliminates the leading FV corrections to both quantities. We re-emphasize that ultimately, one wants to extract as many scattering parameters as feasible from calculations in a single volume, requiring calculations with multiple boosts of the CM as well as multiple arbitrary twists, in order to maximize the inputs to the energy QCs. In general, with arbitrary twist angles, $\phi = (\phi_x, \phi_y, \phi_z)$, the 27×27 matrix representation of the QC matrix cannot be block diagonalized and it has 27 distinct eigenvalues. The truncation to the 3×3 matrices given

¹⁰ In the limit where $\epsilon_1 = 0$, the $J = 1$ α -wave is entirely S-wave, while the β -wave is entirely D-wave. This approximation neglects FV effects of the form $\epsilon_1 e^{-\kappa L}/L$.

in Eq. (18) remains valid, as do the estimates of the truncation errors, but this truncated QC will provide three distinct energy eigenvalues.

While not the focus of this work, it is worth reminding ourselves about the behavior of the positive-energy states in the FV, such as the higher states associated with the 3S_1 - 3D_1 coupled channel or those associated with the 1S_0 np channel, as described in Eq. (8). For an arbitrary twist, the non-interacting energy levels in the FV are determined by integer triplets and the twist angles. Interactions will produce deviations from these non-interacting levels, that become smaller as the lattice volume increases, scaling with $\sim \tan \delta(p^*)/(ML^2)$. As discussed previously, as there is no underlying symmetry for arbitrary twists, the eigenstates will, in general, be non degenerate.

IV. SUMMARY AND CONCLUSIONS

Twisted boundary conditions have been successfully used in numerical calculations of important observables, both in nuclear and particle physics with Lattice QCD, as well as in others areas such as condensed-matter physics. They provide a means with which to select the phase space of particles in a given finite volume, beyond that allowed by periodic or anti-periodic boundary conditions. In LQCD calculations, TBCs have been used to resolve the threshold region required in the evaluation of transition matrix elements without requiring large lattice volumes [21–28, 82]. They can also be used in calculations of elastic $2 \rightarrow 2$ processes by providing a better sampling of CM kinematics in a single volume, allowing for better constraints on scattering parameters [57–60]. In this paper, we have explored the use of TBCs in calculating the mass of single baryons, and in determining the binding of two-hadron systems in a FV, with a focus on the deuteron. In particular, we have used experimentally known scattering data to determine the location of the lowest-lying FV states that have overlap with the deuteron for a selection of twist angles, and combinations thereof. We have found that twisting provides an effective way of exponentially reducing the impact of the finite lattice volume on the calculation of two-body binding energies. Pair-wise combining results obtained with particular twists, such as PBCs and APBCs, can eliminate the leading volume dependence. The same is true for twist averaging, but the uncertainty resulting from a finite number of randomly selected twists can be large. Importantly, we have determined that the i-PBCs, with $\phi = (\frac{\pi}{2}, \frac{\pi}{2}, \frac{\pi}{2})$, eliminate the first three FV corrections to the dominant S-wave contribution to the two-hadron binding energies, suppressing such effects from $\mathcal{O}(e^{-\kappa L}/L)$ to $\mathcal{O}(e^{-2\kappa L}/L)$, while also reducing the FV modifications to the nucleon mass, of the form $\mathcal{O}(e^{-m_\pi L}/L)$, by a factor of three. This translates into at least an order of magnitude improvement in the accuracy of the deuteron binding energy extracted from LQCD correlation functions in volumes as small as $\sim (9 \text{ fm})^3$. As partially-TBCs modify the nuclear forces by terms of order $\mathcal{O}(e^{-m_\pi L}/L)$, such calculations of the deuteron and other bound states can be performed without the need for multiple ensembles of gauge-field configurations, significantly reducing the required computational resources.

Given the generalized Lüscher FV formalism for NN systems [56] with TBCs, not only can the binding energy of the deuteron be obtained from the upcoming LQCD calculations, but the relevant scattering parameters, including the S-D mixing parameter, can be well constrained. While giving different twists to the up and down quarks modifies the neutron and proton phase space in different ways that allows for a parametric reduction in volume effects to the deuteron binding energy, and control on the location of the positive-energy scattering states, it does not change the CM phase space in the neutron-neutron or proton-proton systems. Therefore, it is not a useful tool in refining calculations of scattering parameters in these channels.

Inspired by the volume improvement seen in the QMC calculations of few and many-body systems with twist-averaged BCs [33, 67–70], and studies of Dirichlet BCs and PBCs in QMC and Density-Functional Theory, e.g. Refs. [83, 84], and considering the twist-phase modifications

to the images associated with a given system, we speculate that the FV modifications to the spectrum of three-nucleon and multi-nucleon systems can be reduced by TBCs. The magnitude of the improvement will depend upon the inter-particle forces being short ranged compared to the extent of the system. Due to the complexity of such systems, particularly in a FV [53–55], a definitive conclusion can only be arrived at upon further investigation.

Acknowledgments

We would like to thank W. Nazarewicz, S. Reddy, and other attendees of the INT program *Quantitative Large Amplitude Shape Dynamics: Fission and Heavy-Ion Fusion* (September–November 2013), for stimulating discussions. RB acknowledges support from the US DOE contract DE-AC05-06OR23177, under which Jefferson Science Associates, LLC, manages and operates the Jefferson Laboratory. The work of TL was supported by the DFG through SFB/TR 16 and SFG 634. ZD and MJS were supported in part by DOE grant No. DE-FG02-00ER41132.

-
- [1] A. S. Kronfeld, *Ann.Rev.Nucl.Part.Sci.* **62**, 265 (2012), 1203.1204.
 - [2] A. S. Kronfeld, *ArXiv e-prints* (2012), 1209.3468.
 - [3] S. R. Beane et al. (NPLQCD Collaboration), *Phys.Rev.Lett.* **106**, 162001 (2011), 1012.3812.
 - [4] S. R. Beane, E. Chang, W. Detmold, B. Joo, H. Lin, et al., *Mod.Phys.Lett.* **A26**, 2587 (2011), 1103.2821.
 - [5] T. Inoue et al. (HAL QCD Collaboration), *Phys.Rev.Lett.* **106**, 162002 (2011), 1012.5928.
 - [6] T. Inoue et al. (HAL QCD Collaboration), *Nucl.Phys.* **A881**, 28 (2012), 1112.5926.
 - [7] S. R. Beane et al. (NPLQCD Collaboration), *Phys.Rev.* **D85**, 054511 (2012), 1109.2889.
 - [8] S. R. Beane et al., *Phys.Rev.* **D87**, 034506 (2013), 1206.5219.
 - [9] T. Yamazaki, K.-I. Ishikawa, Y. Kuramashi, and A. Ukawa, *Phys.Rev.* **D86**, 074514 (2012), 1207.4277.
 - [10] T. Yamazaki, K.-I. Ishikawa, Y. Kuramashi, and A. Ukawa (2013), 1310.5797.
 - [11] N. Barnea, L. Contessi, D. Gazit, F. Pederiva, and U. van Kolck (2013), 1311.4966.
 - [12] S. R. Beane et al. (NPLQCD Collaboration), *Phys.Rev.* **D85**, 034505 (2012), 1107.5023.
 - [13] J. J. Dudek, R. G. Edwards, and C. E. Thomas, *Phys.Rev.* **D86**, 034031 (2012), 1203.6041.
 - [14] M. Luscher, *Commun.Math.Phys.* **104**, 177 (1986).
 - [15] M. Luscher, *Nucl.Phys.* **B354**, 531 (1991).
 - [16] S. R. Beane, P. F. Bedaque, A. Parreno, and M. J. Savage, *Phys.Lett.* **B585**, 106 (2004), hep-lat/0312004.
 - [17] Z. Davoudi and M. J. Savage, *Phys.Rev.* **D84**, 114502 (2011), 1108.5371.
 - [18] R. A. Briceno, Z. Davoudi, T. Luu, and M. J. Savage (2013), 1309.3556.
 - [19] N. Byers and C. N. Yang, *Phys. Rev. Lett.* **7**, 46 (1961).
 - [20] P. F. Bedaque, *Phys.Lett.* **B593**, 82 (2004), nucl-th/0402051.
 - [21] B. C. Tiburzi, *Phys.Lett.* **B617**, 40 (2005), hep-lat/0504002.
 - [22] F.-J. Jiang and B. Tiburzi, *Phys.Lett.* **B645**, 314 (2007), hep-lat/0610103.
 - [23] P. Boyle, J. Flynn, A. Juttner, C. Sachrajda, and J. Zanotti, *JHEP* **0705**, 016 (2007), hep-lat/0703005.
 - [24] S. Simula (ETMC Collaboration), *PoS LAT2007*, 371 (2007), 0710.0097.
 - [25] P. Boyle, J. Flynn, A. Juttner, C. Kelly, H. P. de Lima, et al., *JHEP* **0807**, 112 (2008), 0804.3971.
 - [26] S. Aoki, R. Horsley, T. Izubuchi, Y. Nakamura, D. Pleiter, et al. (2008), 0808.1428.
 - [27] P. A. Boyle, J. M. Flynn, A. Juttner, C. Sachrajda, K. Sivalingam, et al., *PoS LATTICE2012*, 112 (2012), 1212.3188.
 - [28] B. B. Brandt, A. Juttner, and H. Wittig, *PoS ConfinementX*, 112 (2012), 1301.3513.
 - [29] G. M. de Divitiis and N. Tantalo (2004), hep-lat/0409154.
 - [30] C. Sachrajda and G. Villadoro, *Phys.Lett.* **B609**, 73 (2005), hep-lat/0411033.
 - [31] C. Gros, *Zeitschrift fur Physik B Condensed Matter* **86**, 359 (1992), ISSN 0722-3277.
 - [32] C. Gros, *Phys. Rev. B* **53**, 6865 (1996).
 - [33] C. Lin, F. H. Zong, and D. M. Ceperley, *Phys. Rev. E* **64**, 016702 (2001), cond-mat/0101339.

- [34] P. F. Bedaque and J.-W. Chen, Phys.Lett. **B616**, 208 (2005), hep-lat/0412023.
- [35] M. Luscher, Commun.Math.Phys. **105**, 153 (1986).
- [36] K. Rummukainen and S. A. Gottlieb, Nucl.Phys. **B450**, 397 (1995), hep-lat/9503028.
- [37] W. Detmold and M. J. Savage, Nucl.Phys. **A743**, 170 (2004), hep-lat/0403005.
- [38] X. Feng, X. Li, and C. Liu, Phys.Rev. **D70**, 014505 (2004), hep-lat/0404001.
- [39] C. Kim, C. Sachrajda, and S. R. Sharpe, Nucl.Phys. **B727**, 218 (2005), hep-lat/0507006.
- [40] N. H. Christ, C. Kim, and T. Yamazaki, Phys.Rev. **D72**, 114506 (2005), hep-lat/0507009.
- [41] C. Liu, X. Feng, and S. He, Int.J.Mod.Phys. **A21**, 847 (2006), hep-lat/0508022.
- [42] S. He, X. Feng, and C. Liu, JHEP **0507**, 011 (2005), hep-lat/0504019.
- [43] V. Bernard, M. Lage, U.-G. Meissner, and A. Rusetsky, JHEP **0808**, 024 (2008), 0806.4495.
- [44] M. Lage, U.-G. Meissner, and A. Rusetsky, Phys.Lett. **B681**, 439 (2009), 0905.0069.
- [45] N. Ishizuka, PoS **LAT2009**, 119 (2009), 0910.2772.
- [46] Z. Fu, Phys.Rev. **D85**, 014506 (2012), 1110.0319.
- [47] S. Bour, S. Koenig, D. Lee, H.-W. Hammer, and U.-G. Meissner, Phys.Rev. **D84**, 091503 (2011), 1107.1272.
- [48] P. Guo, J. Dudek, R. Edwards, and A. P. Szczepaniak, Phys.Rev. **D88**, 014501 (2013), 1211.0929.
- [49] N. Li and C. Liu, Phys.Rev. **D87**, 014502 (2013), 1209.2201.
- [50] L. Leskovec and S. Prelovsek, Phys.Rev. **D85**, 114507 (2012), 1202.2145.
- [51] M. T. Hansen and S. R. Sharpe, Phys.Rev. **D86**, 016007 (2012), 1204.0826.
- [52] R. A. Briceno and Z. Davoudi, Phys. Rev. D. **88**, **094507** (2013), 1204.1110.
- [53] K. Polejaeva and A. Rusetsky, Eur.Phys.J. **A48**, 67 (2012), 1203.1241.
- [54] R. A. Briceno and Z. Davoudi, Phys.Rev. **D87**, 094507 (2013), 1212.3398.
- [55] M. T. Hansen and S. R. Sharpe (2013), 1311.4848.
- [56] R. A. Briceno, Z. Davoudi, and T. C. Luu, Phys.Rev. **D88**, 034502 (2013), 1305.4903.
- [57] V. Bernard, M. Lage, U.-G. Meissner, and A. Rusetsky, JHEP **1101**, 019 (2011), 1010.6018.
- [58] M. Doring, U.-G. Meissner, E. Oset, and A. Rusetsky, Eur.Phys.J. **A47**, 139 (2011), 1107.3988.
- [59] M. Doring, U. Meissner, E. Oset, and A. Rusetsky, Eur.Phys.J. **A48**, 114 (2012), 1205.4838.
- [60] S. Ozaki and S. Sasaki, Phys.Rev. **D87**, 014506 (2013), 1211.5512.
- [61] S. R. Beane, W. Detmold, K. Orginos, and M. J. Savage, Prog.Part.Nucl.Phys. **66**, 1 (2011), 1004.2935.
- [62] S. Prelovsek, L. Leskovec, and D. Mohler (2013), 1310.8127.
- [63] A. Ali Khan et al. (QCDSF-UKQCD Collaboration), Nucl.Phys. **B689**, 175 (2004), hep-lat/0312030.
- [64] S. R. Beane, Phys.Rev. **D70**, 034507 (2004), hep-lat/0403015.
- [65] S. R. Beane, E. Chang, W. Detmold, H. Lin, T. Luu, et al., Phys.Rev. **D84**, 014507 (2011), 1104.4101.
- [66] F.-J. Jiang and B. Tiburzi, Phys.Rev. **D78**, 114505 (2008), 0810.1495.
- [67] G. Rajagopal, R. J. Needs, S. Kenny, W. M. C. Foulkes, and A. James, Phys. Rev. Lett. **73**, 1959 (1994).
- [68] G. Rajagopal, R. J. Needs, A. James, S. D. Kenny, and W. M. C. Foulkes, Phys. Rev. B **51**, 10591 (1995).
- [69] L. M. Fraser, W. M. C. Foulkes, G. Rajagopal, R. J. Needs, S. D. Kenny, and A. J. Williamson, Phys. Rev. B **53**, 1814 (1996).
- [70] W. Wilcox, Annals Phys. **279**, 65 (2000), hep-lat/9909156.
- [71] I. Sato and P. F. Bedaque, Phys.Rev. **D76**, 034502 (2007), hep-lat/0702021.
- [72] D. Agadjanov, U.-G. Meissner, and A. Rusetsky (2013), 1310.7183.
- [73] <http://nn-online.org>, Nijmegen Phase Shift Analysis.
- [74] V. G. J. Stoks, R. A. M. Klomp, M. C. M. Rentmeester, and J. J. de Swart, Phys. Rev. C **48**, 792 (1993).
- [75] V. G. J. Stoks, R. A. M. Klomp, C. P. F. Terheggen, and J. J. de Swart, Phys. Rev. C **49**, 2950 (1994).
- [76] T. A. Rijken and V. G. J. Stoks, Phys. Rev. C **54**, 2851 (1996).
- [77] T. A. Rijken and V. G. J. Stoks, Phys. Rev. C **54**, 2869 (1996).
- [78] J. M. Blatt and L. Biedenharn, Phys.Rev. **86**, 399 (1952).
- [79] M. S. Dresselhaus, G. Dresselhaus, and A. Jorio, *Applications of Group Theory to the Physics of Solids* (Springer, 2008), 1st ed.
- [80] M. Gockeler, R. Horsley, M. Lage, U.-G. Meissner, P. Rakow, et al., Phys.Rev. **D86**, 094513 (2012), 1206.4141.
- [81] C. E. Thomas, R. G. Edwards, and J. J. Dudek, Phys.Rev. **D85**, 014507 (2012), 1107.1930.

- [82] P. A. Boyle, J. M. Flynn, N. Garron, A. Juttner, C. T. Sachrajda, et al., JHEP **1308**, 132 (2013), 1305.7217.
- [83] A. Bulgac and M. M. Forbes, Phys.Rev. **C87**, 051301 (2013), 1301.7354.
- [84] J. Erler, C. Horowitz, W. Nazarewicz, M. Rafalski, and P.-G. Reinhard (2012), 1211.6292.

Appendix A: Twisted Images

It is helpful to make explicit the sums over the twist phases. Consider the sum

$$S(\phi) = \sum_{\mathbf{n} \neq \mathbf{0}} \frac{e^{-|\mathbf{n}|m_\pi L}}{|\mathbf{n}|} e^{-i\mathbf{n} \cdot \phi} \quad , \quad (\text{A1})$$

of which the first few terms are

$$\begin{aligned} S(\phi) &= 2 e^{-m_\pi L} (\cos \phi_x + \cos \phi_y + \cos \phi_z) \\ &+ 2\sqrt{2} e^{-\sqrt{2}m_\pi L} (\cos \phi_x \cos \phi_y + \cos \phi_x \cos \phi_z + \cos \phi_y \cos \phi_z) \\ &+ \frac{8}{\sqrt{3}} e^{-\sqrt{3}m_\pi L} \cos \phi_x \cos \phi_y \cos \phi_z \\ &+ e^{-2m_\pi L} (\cos 2\phi_x + \cos 2\phi_y + \cos 2\phi_z) + \dots \quad . \end{aligned} \quad (\text{A2})$$

For PBCs, with $\phi = (0, 0, 0)$, the first few terms in the sum in Eq. (A1) and (A4) are

$$S(\mathbf{0}) = 6 e^{-m_\pi L} + 6\sqrt{2} e^{-\sqrt{2}m_\pi L} + \frac{8}{\sqrt{3}} e^{-\sqrt{3}m_\pi L} + 3 e^{-2m_\pi L} + \dots \quad , \quad (\text{A3})$$

while for APBs, with $\phi = (\pi, \pi, \pi)$, the sum becomes

$$S(\boldsymbol{\pi}) = -6 e^{-m_\pi L} + 6\sqrt{2} e^{-\sqrt{2}m_\pi L} - \frac{8}{\sqrt{3}} e^{-\sqrt{3}m_\pi L} + 3 e^{-2m_\pi L} - \dots \quad . \quad (\text{A4})$$

It is obvious that the leading terms vanish in the average, with $(S(\mathbf{0}) + S(\boldsymbol{\pi}))/2 = 6\sqrt{2} e^{-\sqrt{2}m_\pi L} + \dots$. A particularly interesting twist is $\phi = (\frac{\pi}{2}, \frac{\pi}{2}, \frac{\pi}{2})$, induced by i-PBCs, for which the first three terms in the sum vanish, leaving

$$S(\frac{\boldsymbol{\pi}}{2}) = -3 e^{-2m_\pi L} + \dots \quad . \quad (\text{A5})$$

Finally, twist averaging this function gives

$$\langle S(\phi) \rangle_\phi = \int \frac{d^3\phi}{(2\pi)^3} S(\phi) = 0 \quad . \quad (\text{A6})$$

Appendix B: Quantization Conditions

The NN FV QCs in the channels that have an overlap with the 3S_1 - 3D_1 coupled channels are listed in this appendix for a selection of twist angles. With the notation of Ref. [56], the QC for the irrep Γ_i can be written as

$$\det \left(\mathbb{M}^{(\Gamma_i)} + i \frac{p^*}{8\pi E^*} - \mathcal{F}^{(\Gamma_i), \mathbf{d}, \phi_1, \phi_2} \right) = 0 \quad , \quad (\text{B1})$$

where

$$\begin{aligned} \mathcal{F}^{(\Gamma_i), \mathbf{d}, \phi_1, \phi_2}(p^{*2}; L) &= \frac{1}{2E^*} \sum_{l,m} \frac{1}{p^{*l}} \mathbb{F}_{lm}^{(\Gamma_i)} c_{lm}^{\mathbf{d}, \phi_1, \phi_2}(p^{*2}; L) \quad , \\ \mathbb{M}^{(\Gamma_i)} &= (\mathcal{M}^{-1})_{\Gamma_i} \quad . \end{aligned} \quad (\text{B2})$$

where $c_{lm}^{\mathbf{d},\phi_1,\phi_2}(p^{*2};L)$ functions are defined in Eqs. (10),(11) and (16), E^* is NN CM energy and p^* is the on-shell momentum of each nucleon in the CM frame.¹¹ In the summation over “ m ” in Eq. (B2), only the $\mathbb{F}_{lm}^{(\Gamma_i)}$ listed below are included as the other contributions have already been summed using the symmetries of the systems. In the following we set $\phi_1 = -\phi_2 = \phi$. It is straightforward to decompose \mathcal{M}^{-1} into $(\mathcal{M}^{-1})_{\Gamma_i}$ using the eigenvectors of the FV functions [13, 81]. For notational convenience, $\mathcal{M}_{J,L}$ denotes the scattering amplitude in the channel with total angular momentum J and orbital angular momentum L . $\mathcal{M}_{1,SD}$ is the amplitude between S and D partial waves in the $J = 1$ channel, and $\det \mathcal{M}_1$ is the determinant of the $J = 1$ sector of the scattering-amplitude matrix,

$$\det \mathcal{M}_1 = \det \begin{pmatrix} \mathcal{M}_{1,S} & \mathcal{M}_{1,SD} \\ \mathcal{M}_{1,DS} & \mathcal{M}_{1,D} \end{pmatrix} . \quad (\text{B3})$$

1. $\phi = (0, 0, 0)$

$$\mathbb{T}_1 : \quad \mathbb{F}_{00}^{(\mathbb{T}_1)} = \mathbf{I}_3, \quad \mathbb{F}_{40}^{(\mathbb{T}_1)} = \begin{pmatrix} 0 & 0 & 0 \\ 0 & 0 & \frac{2\sqrt{6}}{7} \\ 0 & \frac{2\sqrt{6}}{7} & \frac{2}{7} \end{pmatrix}, \quad \mathbb{M}^{(\mathbb{T}_1)} = \begin{pmatrix} \frac{\mathcal{M}_{1,D}}{\det \mathcal{M}_1} & -\frac{\mathcal{M}_{1,SD}}{\det \mathcal{M}_1} & 0 \\ -\frac{\mathcal{M}_{1,SD}}{\det \mathcal{M}_1} & \frac{\mathcal{M}_{1,S}}{\det \mathcal{M}_1} & 0 \\ 0 & 0 & \mathcal{M}_{3,D}^{-1} \end{pmatrix} . \quad (\text{B4})$$

2. $\phi = (\frac{\pi}{2}, \frac{\pi}{2}, \frac{\pi}{2})$

$$\begin{aligned} \mathbb{A}_2 : \quad \mathbb{F}_{00}^{(\mathbb{A}_2)} = \mathbf{I}_6, \quad \mathbb{F}_{10}^{(\mathbb{A}_2)} = \begin{pmatrix} 0 & -1 & \sqrt{2} & 0 & 0 & 0 \\ -1 & 0 & 0 & \sqrt{2} & 0 & 0 \\ \sqrt{2} & 0 & 0 & -\frac{1}{5} & 0 & 0 \\ 0 & \sqrt{2} & -\frac{1}{5} & 0 & \frac{3\sqrt{6}}{5} & 0 \\ 0 & 0 & 0 & \frac{3\sqrt{6}}{5} & 0 & 0 \\ 0 & 0 & 0 & 0 & 0 & 0 \end{pmatrix}, \quad \mathbb{F}_{22}^{(\mathbb{A}_2)} = i \times \begin{pmatrix} 0 & 0 & 0 & 2\sqrt{\frac{3}{5}} & 0 & 0 \\ 0 & 0 & 2\sqrt{\frac{3}{5}} & 0 & -3\sqrt{\frac{2}{5}} & 0 \\ 0 & 2\sqrt{\frac{3}{5}} & -\sqrt{\frac{6}{5}} & 0 & \frac{6}{7\sqrt{5}} & 0 \\ 2\sqrt{\frac{3}{5}} & 0 & 0 & -\sqrt{\frac{6}{5}} & 0 & 0 \\ 0 & -3\sqrt{\frac{2}{5}} & \frac{6}{7\sqrt{5}} & 0 & -\frac{8}{7}\sqrt{\frac{6}{5}} & 0 \\ 0 & 0 & 0 & 0 & 0 & \frac{2\sqrt{30}}{7} \end{pmatrix}, \\ \\ \mathbb{F}_{30}^{(\mathbb{A}_2)} = \begin{pmatrix} 0 & 0 & 0 & 0 & \frac{2}{\sqrt{7}} & \sqrt{\frac{5}{7}} \\ 0 & 0 & 0 & 0 & 0 & 0 \\ 0 & 0 & 0 & \frac{6\sqrt{\frac{3}{7}}}{5} & 0 & 0 \\ 0 & 0 & \frac{6\sqrt{\frac{3}{7}}}{5} & 0 & -\frac{4\sqrt{\frac{2}{7}}}{5} & \sqrt{\frac{5}{14}} \\ \frac{2}{\sqrt{7}} & 0 & 0 & -\frac{4\sqrt{\frac{2}{7}}}{5} & 0 & 0 \\ \sqrt{\frac{5}{7}} & 0 & 0 & \sqrt{\frac{5}{14}} & 0 & 0 \end{pmatrix}, \quad \mathbb{F}_{32}^{(\mathbb{A}_2)} = i \times \begin{pmatrix} 0 & 0 & 0 & 0 & \sqrt{\frac{10}{21}} & -2\sqrt{\frac{2}{21}} \\ 0 & 0 & 0 & 0 & 0 & 0 \\ 0 & 0 & 0 & 3\sqrt{\frac{2}{35}} & 0 & 0 \\ 0 & 0 & 3\sqrt{\frac{2}{35}} & 0 & -\frac{4}{\sqrt{105}} & -\frac{2}{\sqrt{21}} \\ \sqrt{\frac{10}{21}} & 0 & 0 & -\frac{4}{\sqrt{105}} & 0 & 0 \\ -2\sqrt{\frac{2}{21}} & 0 & 0 & -\frac{2}{\sqrt{21}} & 0 & 0 \end{pmatrix}, \end{aligned}$$

¹¹ The relativistic normalization of states has been used such that for a single S-wave channel with phase shift δ , the scattering amplitude is $\mathcal{M} = \frac{8\pi E^*}{p^*} \frac{(e^{2i\delta} - 1)}{2i}$.

$$\begin{aligned}
\mathbb{F}_{40}^{(A_2)} &= \begin{pmatrix} 0 & 0 & 0 & 0 & 0 & 0 \\ 0 & 0 & 0 & 0 & 0 & 0 \\ 0 & 0 & 0 & 0 & \frac{4\sqrt{\frac{2}{3}}}{7} & \frac{2\sqrt{\frac{10}{3}}}{7} \\ 0 & 0 & 0 & 0 & 0 & 0 \\ 0 & 0 & \frac{4\sqrt{\frac{2}{3}}}{7} & 0 & -\frac{4}{21} & \frac{4\sqrt{5}}{21} \\ 0 & 0 & \frac{2\sqrt{\frac{10}{3}}}{7} & 0 & \frac{4\sqrt{5}}{21} & -\frac{2}{21} \end{pmatrix}, \quad \mathbb{F}_{42}^{(A_2)} = i \times \begin{pmatrix} 0 & 0 & 0 & 0 & 0 & 0 \\ 0 & 0 & 0 & 0 & 0 & 0 \\ 0 & 0 & 0 & 0 & \frac{8}{7}\sqrt{\frac{5}{3}} & -\frac{1}{\sqrt{3}} \\ 0 & 0 & 0 & 0 & 0 & 0 \\ 0 & 0 & \frac{8}{7}\sqrt{\frac{5}{3}} & 0 & -\frac{4\sqrt{10}}{21} & -\frac{\sqrt{2}}{3} \\ 0 & 0 & -\frac{1}{\sqrt{3}} & 0 & -\frac{\sqrt{2}}{3} & -\frac{2\sqrt{10}}{21} \end{pmatrix}, \\
\mathbb{M}^{(A_2)} &= \begin{pmatrix} \mathcal{M}_{0,P}^{-1} & 0 & 0 & 0 & 0 & 0 \\ 0 & \frac{\mathcal{M}_{1,D}}{\det \mathcal{M}_1} & -\frac{\mathcal{M}_{1,SD}}{\det \mathcal{M}_1} & 0 & 0 & 0 \\ 0 & -\frac{\mathcal{M}_{1,SD}}{\det \mathcal{M}_1} & \frac{\mathcal{M}_{1,S}}{\det \mathcal{M}_1} & 0 & 0 & 0 \\ 0 & 0 & 0 & \mathcal{M}_{2,P}^{-1} & 0 & 0 \\ 0 & 0 & 0 & 0 & \mathcal{M}_{3,D}^{-1} & 0 \\ 0 & 0 & 0 & 0 & 0 & \mathcal{M}_{3,D}^{-1} \end{pmatrix}. \tag{B5}
\end{aligned}$$

$$\begin{aligned}
\mathbb{E}: \quad \mathbb{F}_{00}^{(\mathbb{E})} &= \mathbf{I}_9, \quad \mathbb{F}_{10}^{(\mathbb{E})} = \begin{pmatrix} 0 & \sqrt{\frac{3}{2}} & 0 & 0 & \sqrt{\frac{3}{2}} & 0 & 0 & 0 & 0 \\ \sqrt{\frac{3}{2}} & 0 & \frac{\sqrt{3}}{2} & 0 & 0 & 0 & \frac{3\sqrt{\frac{3}{2}}}{2} & 0 & 0 \\ 0 & \frac{\sqrt{3}}{2} & 0 & 0 & -\frac{\sqrt{3}}{10} & 0 & 0 & 0 & 0 \\ 0 & 0 & 0 & 0 & 0 & \sqrt{\frac{3}{5}} & 0 & \sqrt{\frac{6}{5}} & 0 \\ \sqrt{\frac{3}{2}} & 0 & -\frac{\sqrt{3}}{10} & 0 & 0 & 0 & \frac{\sqrt{\frac{3}{5}}}{2} & 0 & \frac{4\sqrt{3}}{5} \\ 0 & 0 & 0 & \sqrt{\frac{3}{5}} & 0 & 0 & 0 & 0 & 0 \\ 0 & \frac{3\sqrt{\frac{3}{5}}}{2} & 0 & 0 & \frac{\sqrt{\frac{3}{5}}}{2} & 0 & 0 & 0 & 0 \\ 0 & 0 & 0 & \sqrt{\frac{6}{5}} & 0 & 0 & 0 & 0 & 0 \\ 0 & 0 & 0 & 0 & \frac{4\sqrt{3}}{5} & 0 & 0 & 0 & 0 \end{pmatrix}, \\
\mathbb{F}_{22}^{(\mathbb{E})} &= i \times \begin{pmatrix} 0 & 0 & -\sqrt{\frac{3}{5}} & 0 & 0 & 0 & -\sqrt{3} & 0 & -2\sqrt{\frac{3}{5}} \\ 0 & -\sqrt{\frac{3}{10}} & 0 & 0 & -3\sqrt{\frac{3}{10}} & 0 & 0 & 0 & 0 \\ -\sqrt{\frac{3}{5}} & 0 & \sqrt{\frac{3}{10}} & 0 & 0 & 0 & -\sqrt{\frac{3}{2}} & 0 & \frac{2}{7}\sqrt{\frac{6}{5}} \\ 0 & 0 & 0 & \sqrt{\frac{6}{5}} & 0 & 0 & 0 & 0 & 0 \\ 0 & -3\sqrt{\frac{3}{10}} & 0 & 0 & -\sqrt{\frac{3}{10}} & 0 & 0 & 0 & 0 \\ 0 & 0 & 0 & 0 & 0 & \frac{\sqrt{30}}{7} & 0 & -\frac{2\sqrt{15}}{7} & 0 \\ -\sqrt{3} & 0 & -\sqrt{\frac{3}{2}} & 0 & 0 & 0 & -\frac{1}{7}\sqrt{\frac{15}{2}} & 0 & -\frac{2\sqrt{6}}{7} \\ 0 & 0 & 0 & 0 & 0 & -\frac{2\sqrt{15}}{7} & 0 & 0 & 0 \\ -2\sqrt{\frac{3}{5}} & 0 & \frac{2}{7}\sqrt{\frac{6}{5}} & 0 & 0 & 0 & -\frac{2\sqrt{6}}{7} & 0 & -\frac{6}{7}\sqrt{\frac{6}{5}} \end{pmatrix}, \\
\mathbb{F}_{30}^{(\mathbb{E})} &= \begin{pmatrix} 0 & 0 & 0 & 0 & 0 & 0 & 0 & 0 & 0 \\ 0 & 0 & 0 & 0 & 0 & -\sqrt{\frac{5}{14}} & -\frac{2}{\sqrt{35}} & \frac{\sqrt{\frac{5}{7}}}{2} & -\frac{2}{\sqrt{7}} \\ 0 & 0 & 0 & \frac{3}{\sqrt{14}} & -\frac{6}{5\sqrt{7}} & 0 & 0 & 0 & 0 \\ 0 & 0 & \frac{3}{\sqrt{14}} & 0 & 0 & \frac{2}{\sqrt{35}} & -\sqrt{\frac{5}{14}} & 2\sqrt{\frac{2}{35}} & \frac{1}{\sqrt{14}} \\ 0 & 0 & -\frac{6}{5\sqrt{7}} & 0 & 0 & \sqrt{\frac{5}{14}} & -\frac{4}{\sqrt{35}} & -\frac{\sqrt{\frac{5}{7}}}{2} & -\frac{2}{5\sqrt{7}} \\ 0 & -\sqrt{\frac{5}{14}} & 0 & \frac{2}{\sqrt{35}} & \sqrt{\frac{5}{14}} & 0 & 0 & 0 & 0 \\ 0 & -\frac{2}{\sqrt{35}} & 0 & -\sqrt{\frac{5}{14}} & -\frac{4}{\sqrt{35}} & 0 & 0 & 0 & 0 \\ 0 & \frac{\sqrt{\frac{5}{7}}}{2} & 0 & 2\sqrt{\frac{2}{35}} & -\frac{\sqrt{\frac{5}{7}}}{2} & 0 & 0 & 0 & 0 \\ 0 & -\frac{2}{\sqrt{7}} & 0 & \frac{1}{\sqrt{14}} & -\frac{2}{5\sqrt{7}} & 0 & 0 & 0 & 0 \end{pmatrix},
\end{aligned}$$

$$\begin{aligned}
\mathbb{F}_{32}^{(\mathbb{E})} &= i \times \begin{pmatrix} 0 & 0 & 0 & 0 & 0 & 0 & 0 & 0 & 0 \\ 0 & 0 & 0 & 0 & 0 & \frac{2}{\sqrt{21}} & -\sqrt{\frac{2}{21}} & -\sqrt{\frac{2}{21}} & -\sqrt{\frac{10}{21}} \\ 0 & 0 & 0 & -2\sqrt{\frac{3}{35}} & -\sqrt{\frac{6}{35}} & 0 & 0 & 0 & 0 \\ 0 & 0 & -2\sqrt{\frac{3}{35}} & 0 & 0 & \sqrt{\frac{2}{21}} & \frac{2}{\sqrt{21}} & \frac{2}{\sqrt{21}} & -\sqrt{\frac{105}{21}} \\ 0 & 0 & -\sqrt{\frac{6}{35}} & 0 & 0 & -\frac{2}{\sqrt{21}} & -2\sqrt{\frac{2}{21}} & \sqrt{\frac{2}{21}} & -\sqrt{\frac{2}{105}} \\ 0 & \frac{2}{\sqrt{21}} & 0 & \sqrt{\frac{2}{21}} & -\frac{2}{\sqrt{21}} & 0 & 0 & 0 & 0 \\ 0 & -\sqrt{\frac{2}{21}} & 0 & \frac{2}{\sqrt{21}} & -2\sqrt{\frac{2}{21}} & 0 & 0 & 0 & 0 \\ 0 & -\sqrt{\frac{2}{21}} & 0 & \frac{2}{\sqrt{21}} & \sqrt{\frac{2}{21}} & 0 & 0 & 0 & 0 \\ 0 & -\sqrt{\frac{10}{21}} & 0 & -\frac{2}{\sqrt{105}} & -\sqrt{\frac{2}{105}} & 0 & 0 & 0 & 0 \end{pmatrix}, \\
\mathbb{F}_{40}^{(\mathbb{E})} &= \begin{pmatrix} 0 & 0 & 0 & 0 & 0 & 0 & 0 & 0 & 0 \\ 0 & 0 & 0 & 0 & 0 & 0 & 0 & 0 & 0 \\ 0 & 0 & 0 & 0 & 0 & 0 & \frac{2\sqrt{5}}{7} & -\frac{2}{7} & 0 \\ 0 & 0 & 0 & 0 & 0 & 0 & 0 & 0 & 0 \\ 0 & 0 & 0 & 0 & 0 & 0 & 0 & 0 & 0 \\ 0 & 0 & 0 & 0 & 0 & \frac{4}{63} & -\frac{20\sqrt{2}}{63} & \frac{10\sqrt{2}}{63} & \frac{10\sqrt{10}}{63} \\ 0 & 0 & 0 & 0 & -\frac{20\sqrt{2}}{63} & -\frac{16}{63} & -\frac{10}{63} & -\frac{10\sqrt{5}}{63} & 0 \\ 0 & 0 & \frac{2\sqrt{5}}{7} & 0 & 0 & \frac{10\sqrt{2}}{63} & -\frac{10}{63} & \frac{2}{9} & -\frac{4\sqrt{5}}{63} \\ 0 & 0 & -\frac{2}{7} & 0 & 0 & \frac{10\sqrt{10}}{63} & -\frac{10\sqrt{5}}{63} & -\frac{4\sqrt{5}}{63} & -\frac{2}{63} \end{pmatrix}, \quad \mathbb{F}_{42}^{(\mathbb{E})} = i \times \begin{pmatrix} 0 & 0 & 0 & 0 & 0 & 0 & 0 & 0 & 0 \\ 0 & 0 & 0 & 0 & 0 & 0 & 0 & 0 & 0 \\ 0 & 0 & 0 & 0 & 0 & 0 & 0 & -\frac{1}{\sqrt{2}} & -\frac{2\sqrt{10}}{7} \\ 0 & 0 & 0 & 0 & 0 & 0 & 0 & 0 & 0 \\ 0 & 0 & 0 & 0 & 0 & 0 & 0 & 0 & 0 \\ 0 & 0 & 0 & 0 & 0 & \frac{4\sqrt{10}}{63} & \frac{2\sqrt{5}}{9} & \frac{20\sqrt{5}}{63} & -\frac{5}{9} \\ 0 & 0 & 0 & 0 & \frac{2\sqrt{5}}{9} & -\frac{16\sqrt{10}}{63} & \frac{1}{9}\sqrt{\frac{5}{2}} & -\frac{50\sqrt{2}}{63} \\ 0 & 0 & -\frac{1}{\sqrt{2}} & 0 & 0 & \frac{20\sqrt{5}}{63} & \frac{1}{9}\sqrt{\frac{5}{2}} & \frac{2\sqrt{10}}{9} & \frac{\sqrt{2}}{9} \\ 0 & 0 & -\frac{2\sqrt{10}}{7} & 0 & 0 & -\frac{5}{9} & -\frac{50\sqrt{2}}{63} & \frac{\sqrt{2}}{9} & -\frac{2\sqrt{10}}{63} \end{pmatrix}, \\
\mathbb{M}^{(\mathbb{E})} &= \begin{pmatrix} \frac{\mathcal{M}_{1,D}}{\det \mathcal{M}_1} & 0 & -\frac{\mathcal{M}_{1,SD}}{\det \mathcal{M}_1} & 0 & 0 & 0 & 0 & 0 & 0 \\ 0 & \mathcal{M}_{1,P}^{-1} & 0 & 0 & 0 & 0 & 0 & 0 & 0 \\ -\frac{\mathcal{M}_{1,SD}}{\det \mathcal{M}_1} & 0 & \frac{\mathcal{M}_{1,S}}{\det \mathcal{M}_1} & 0 & 0 & 0 & 0 & 0 & 0 \\ 0 & 0 & 0 & \mathcal{M}_{2,P}^{-1} & 0 & 0 & 0 & 0 & 0 \\ 0 & 0 & 0 & 0 & \mathcal{M}_{2,P}^{-1} & 0 & 0 & 0 & 0 \\ 0 & 0 & 0 & 0 & 0 & \mathcal{M}_{2,D}^{-1} & 0 & 0 & 0 \\ 0 & 0 & 0 & 0 & 0 & 0 & \mathcal{M}_{2,D}^{-1} & 0 & 0 \\ 0 & 0 & 0 & 0 & 0 & 0 & 0 & \mathcal{M}_{3,D}^{-1} & 0 \\ 0 & 0 & 0 & 0 & 0 & 0 & 0 & 0 & \mathcal{M}_{3,D}^{-1} \end{pmatrix}. \tag{B6}
\end{aligned}$$

3. $\phi = (\pi, \pi, \pi)$

$$\mathbb{A}_2: \quad \mathbb{F}_{00}^{(\mathbb{A}_2)} = \mathbf{I}_4, \quad \mathbb{F}_{40}^{(\mathbb{A}_2)} = \begin{pmatrix} 0 & 0 & 0 & 0 \\ 0 & 0 & \frac{2\sqrt{6}}{7} & 0 \\ 0 & \frac{2\sqrt{6}}{7} & \frac{2}{7} & 0 \\ 0 & 0 & 0 & -\frac{4}{7} \end{pmatrix}, \quad \mathbb{M}^{(\mathbb{A}_2)} = \begin{pmatrix} \frac{\mathcal{M}_{1,D}}{\det \mathcal{M}_1} & -\frac{\mathcal{M}_{1,SD}}{\det \mathcal{M}_1} & 0 & 0 \\ -\frac{\mathcal{M}_{1,SD}}{\det \mathcal{M}_1} & \frac{\mathcal{M}_{1,S}}{\det \mathcal{M}_1} & 0 & 0 \\ 0 & 0 & \mathcal{M}_{3,D}^{-1} & 0 \\ 0 & 0 & 0 & \mathcal{M}_{3,D}^{-1} \end{pmatrix}. \tag{B7}$$

$$\mathbb{E}: \quad \mathbb{F}_{00}^{(\mathbb{E})} = \mathbf{I}_6, \quad \mathbb{F}_{40}^{(\mathbb{E})} = \begin{pmatrix} 0 & 0 & 0 & 0 & 0 & 0 \\ 0 & 0 & \frac{2\sqrt{6}}{7} & 0 & 0 & 0 \\ 0 & \frac{2\sqrt{6}}{7} & \frac{2}{7} & 0 & 0 & 0 \\ 0 & 0 & 0 & \frac{8}{21} & -\frac{10\sqrt{2}}{21} & 0 \\ 0 & 0 & 0 & -\frac{10\sqrt{2}}{21} & -\frac{2}{21} & 0 \\ 0 & 0 & 0 & 0 & 0 & -\frac{4}{7} \end{pmatrix}, \quad \mathbb{M}^{(\mathbb{E})} = \begin{pmatrix} \frac{\mathcal{M}_{1,D}}{\det \mathcal{M}_1} & -\frac{\mathcal{M}_{1,SD}}{\det \mathcal{M}_1} & 0 & 0 & 0 & 0 \\ -\frac{\mathcal{M}_{1,SD}}{\det \mathcal{M}_1} & \frac{\mathcal{M}_{1,S}}{\det \mathcal{M}_1} & 0 & 0 & 0 & 0 \\ 0 & 0 & \mathcal{M}_{3,D}^{-1} & 0 & 0 & 0 \\ 0 & 0 & 0 & \mathcal{M}_{2,D}^{-1} & 0 & 0 \\ 0 & 0 & 0 & 0 & \mathcal{M}_{3,D}^{-1} & 0 \\ 0 & 0 & 0 & 0 & 0 & \mathcal{M}_{2,D}^{-1} \end{pmatrix}. \tag{B8}$$

Appendix C: Twisted $c_{lm}^{\mathbf{d}, \phi_1, \phi_2}$ Functions for Systems at Rest

To understand the relative contributions of phase shifts beyond the α wave to the deuteron binding energy, it is helpful to consider the expansions of the $c_{lm}^{\mathbf{d}, \phi_1, \phi_2}$ functions. As i-PBCs, with the twist

angles $\phi = (\frac{\pi}{2}, \frac{\pi}{2}, \frac{\pi}{2})$, lead to the most significant reduction in the FV corrections, we focus on these angles in the expansions, restricting ourselves to systems at rest. The general form of the $c_{lm}^{\mathbf{d}, \phi_1, \phi_2}$ functions for $\mathbf{d} = \mathbf{0}$ and $\phi_1 = -\phi_2 = \phi$ is

$$c_{lm}^{\mathbf{0}, \phi, -\phi}(-\kappa^2; L) = \frac{i^l}{\pi^{3/2}} \sum_{\mathbf{n} \neq \mathbf{0}} e^{-i\mathbf{n} \cdot \phi} Y_{lm}(\hat{\mathbf{n}}) \int_0^\infty dk \frac{k^{l+2}}{k^2 + \kappa^2} j_l(n\kappa L) \quad , \quad (C1)$$

where $n = |\mathbf{n}|$. By direct evaluation of the integral, it is straightforward to show that

$$c_{00}^{\mathbf{0}, \phi, -\phi}(-\kappa^2; L) = -\frac{\kappa}{4\pi} + \sqrt{4\pi} \sum_{\mathbf{n} \neq \mathbf{0}} e^{-i\mathbf{n} \cdot \phi} Y_{00}(\hat{\mathbf{n}}) \frac{e^{-n\kappa L}}{4\pi n L} \quad , \quad (C2)$$

$$c_{1m}^{\mathbf{0}, \phi, -\phi}(-\kappa^2; L) = (i\kappa)\sqrt{4\pi} \sum_{\mathbf{n} \neq \mathbf{0}} e^{-i\mathbf{n} \cdot \phi} Y_{1m}(\hat{\mathbf{n}}) \left(1 + \frac{1}{n\kappa L}\right) \frac{e^{-n\kappa L}}{4\pi n L} \quad , \quad (C3)$$

$$c_{2m}^{\mathbf{0}, \phi, -\phi}(-\kappa^2; L) = (i\kappa)^2\sqrt{4\pi} \sum_{\mathbf{n} \neq \mathbf{0}} e^{-i\mathbf{n} \cdot \phi} Y_{2m}(\hat{\mathbf{n}}) \left(1 + \frac{3}{n\kappa L} + \frac{3}{n^2\kappa^2 L^2}\right) \frac{e^{-n\kappa L}}{4\pi n L} \quad , \quad (C4)$$

$$c_{3m}^{\mathbf{0}, \phi, -\phi}(-\kappa^2; L) = (i\kappa)^3\sqrt{4\pi} \sum_{\mathbf{n} \neq \mathbf{0}} e^{-i\mathbf{n} \cdot \phi} Y_{3m}(\hat{\mathbf{n}}) \left(1 + \frac{6}{n\kappa L} + \frac{15}{n^2\kappa^2 L^2} + \frac{15}{n^3\kappa^3 L^3}\right) \frac{e^{-n\kappa L}}{4\pi n L} \quad , \quad (C5)$$

$$c_{4m}^{\mathbf{0}, \phi, -\phi}(-\kappa^2; L) = (i\kappa)^4\sqrt{4\pi} \sum_{\mathbf{n} \neq \mathbf{0}} e^{-i\mathbf{n} \cdot \phi} Y_{4m}(\hat{\mathbf{n}}) \left(1 + \frac{10}{n\kappa L} + \frac{45}{n^2\kappa^2 L^2} + \frac{105}{n^3\kappa^3 L^3} + \frac{105}{n^4\kappa^4 L^4}\right) \frac{e^{-n\kappa L}}{4\pi n L} \quad . \quad (C6)$$

These functions are of the form

$$\begin{aligned} F_{lm} &= \sum_{\mathbf{n} \neq \mathbf{0}} e^{-i\mathbf{n} \cdot \phi} Y_{lm}(\hat{\mathbf{n}}) f(n) \\ &= \alpha_{lm}^{(1)} f(1) + \alpha_{lm}^{(\sqrt{2})} f(\sqrt{2}) + \alpha_{lm}^{(\sqrt{3})} f(\sqrt{3}) + \alpha_{lm}^{(2)} f(2) + \dots \quad . \end{aligned} \quad (C7)$$

The independent and non-vanishing coefficients $\alpha^{(n)}$ are presented in Table I for the twist angles $\phi = (\frac{\pi}{2}, \frac{\pi}{2}, \frac{\pi}{2})$.

(l, m)	$\alpha_{lm}^{(1)}$	$\alpha_{lm}^{(\sqrt{2})}$	$\alpha_{lm}^{(\sqrt{3})}$	$\alpha_{lm}^{(2)}$
(0, 0)	0	0	0	$-\frac{3}{\sqrt{\pi}}$
(1, 0)	$-i\sqrt{\frac{3}{\pi}}$	0	0	0
(2, 2)	0	$-i\sqrt{\frac{15}{2\pi}}$	0	0
(3, 0)	$-i\sqrt{\frac{7}{\pi}}$	0	0	0
(3, 2)	0	0	$-\frac{2}{3}\sqrt{\frac{70}{\pi}}$	0
(4, 0)	0	0	0	$-\frac{21}{4\sqrt{\pi}}$
(4, 2)	0	$i\frac{3}{2}\sqrt{\frac{5}{2\pi}}$	0	0

TABLE I: Coefficients of independent, non-vanishing terms in the expansion of F_{lm} given in Eq. (C7)

The remaining coefficients are dictated by symmetry,

$$\begin{aligned}
F_{1\pm 1} &= \mp e^{\pm i\pi/4} F_{10} \quad , \\
F_{2+2} &= -F_{2-2} = -\frac{1}{\sqrt{2}} e^{\pm i\pi/4} F_{2\pm 1} \quad , \\
F_{30} &= \mp \frac{4}{\sqrt{10}} e^{\pm i\pi/4} F_{3\pm 3} = \pm \frac{4}{\sqrt{6}} e^{\mp i\pi/4} F_{3\pm 1} \quad , \quad F_{3-2} = -F_{3+2} \quad , \\
F_{4+2} &= -F_{4-2} = -\frac{2}{\sqrt{7}} e^{\mp i\pi/4} F_{4\pm 3} = 2e^{\pm i\pi/4} F_{4\pm 1} \quad , \quad F_{40} = \sqrt{\frac{14}{5}} F_{4\pm 4} \quad . \quad (C8)
\end{aligned}$$

The coefficients presented in Table I and Eq. (C8) show that the leading volume dependences of the $c_{lm}^{\mathbf{0},\phi,-\phi}$ functions for i-PBCs are $c_{00} = -\frac{\kappa}{4\pi} + \mathcal{O}(e^{-2\kappa L}/L)$, $c_{10} = \mathcal{O}(e^{-\kappa L}/L)$, $c_{22} = \mathcal{O}(e^{-\sqrt{2}\kappa L}/L)$, $c_{30} = \mathcal{O}(e^{-\kappa L}/L)$, $c_{32} = \mathcal{O}(e^{-\sqrt{3}\kappa L}/L)$, $c_{40} = \mathcal{O}(e^{-2\kappa L}/L)$ and $c_{42} = \mathcal{O}(e^{-\sqrt{2}\kappa L}/L)$. As the P-wave contribution to the FV spectra is due to non-zero c_{1m} and c_{3m} functions, they provide the dominant corrections to the approximate QC in Eq. (18).

A numerical comparison between these expansions and an exact evaluation of the $c_{lm}^{\mathbf{d},\phi_1,\phi_2}$ functions reveals that the expansions are only slowly convergent [18]. Precisions extractions of the energy eigenvalues require the use of the exact evaluations, even in modest volumes.